7.5 SURFACE LAYER TURBULENCE DURING A FRONTAL PASSAGE

Mark Piper, Julie K. Lundquist *

Program in Atmospheric and Oceanic Science, University of Colorado at Boulder

Atmospheric Science Division
Lawrence Livermore National Laboratory, Livermore, CA, 94550

1. INTRODUCTION

Some recent investigations have begun to quantify turbulence and dissipation in frontal zones to address the question of what physical mechanism counteracts the intensification of temperature and velocity gradients across a developing front. Frank (1994) examines the turbulence structure of two fronts that passed a 200m instrumented tower near Karlsruhe, Germany. In addition to showing the mean vertical structure of the fronts as they pass the tower, Frank demonstrates that there is an order of magnitude or more increase in turbulent kinetic energy across the frontal zone. Blumen and Piper (1999) reported turbulence statistics, including dissipation rate measurements, from the MICROFRONTS field experiment, where high-frequency turbulence data were collected from tower-mounted hotwire and sonic anemometers in a cold front and in a density current. Chapman and Browning (2001) measured dissipation rate in a precipitating frontal zone with high-resolution Doppler radar. Their measurements were conducted above the surface layer, to heights of 5km. The dissipation rate values they found are comparable to those measured in Kennedy and Shapiro (1975) in an upper-level front. Here, we expand on these recent studies by depicting the behavior of the fine scales of turbulence near the surface in a frontal zone. The primary objective of this study is to quantify the levels of turbulence and dissipation occurring in a frontal zone through the calculation of kinetic energy spectra and dissipation rates. The high-resolution turbulence data used in this study are taken during the cold front that passed the MICROFRONTS site in the early evening hours of 20 March 1995. These new measurements can be used as a basis for parameterizing the effects of surface-layer turbulence in numerical models of frontogenesis.

We present three techniques for calculating the dissipation rate: direct dissipation technique, inertial dissipation technique and Kolmogorov's four-fifths law. Dissipation rate calculations using these techniques are employed using data from both the sonic and hotwire anemometers, when possible. Unfortunately, direct calculations of ε were not possible during a part of the frontal passage because the high wind speeds concurrent with the frontal passage demand very high frequency resolution, beyond that possible with the hotwire anemometer, for direct ε calculations. The calculations resulting from these three techniques are presented for the cold front as a time series. Quantitative comparisons of the direct and indirect calculation techniques are also given. More detail, as well as a discussion of energy spectra, can be found in Piper & Lundquist (2004).

2. DATA SOURCES

The MICROFRONTS field experiment was conducted from 1 March 1995 through 30 March 1995 at a site approximately 75~km northeast of Wichita, near De Graff, Kansas. The field site was situated in gently rolling farmland in eastern Kansas, with a homogeneous fetch to the northwest. The ASTER facility, operated by the National Center for Atmospheric Research (NCAR) Atmospheric Technology Division, was deployed to collect turbulence data. The ASTER sonic anemometers were used to compute turbulence statistics for the three velocity components and used to estimate dissipation rate.

In addition to sonic anemometers and other standard instrumentation in ASTER, a constant-temperature hotwire anemometer was deployed at 3 m on the south tower to make fine scale wind measurements and to directly measure dissipation rate ε. This hotwire, a TSI model 1210-T1.5 with a 1.3-mm long, 4μm diameter tungsten wire, was oriented vertically to measure the horizontal component of the wind, and aligned at 315 degrees from north to coincide with the climatologically preferred direction of frontal passages at the site.

Owing to the long run times of the hotwire in the MICROFRONTS experiment (continuous operation for several days), an *in situ* calibration of the MICROFRONTS anemometers using wind speed data from the collocated sonic anemometer

at 3m was needed. The calibration was performed using King's Law, as described in detail in Piper & Lundquist (2004). This technique was successfully used by Oncley et al. (1996) and as a check on the hotwires used by Champagne (1978).

For direct dissipation calculations, all scales which experience dissipation must be resolved. As wind speeds during the frontal passage reached 12 ms^{-1}, the Kolmogorov frequency f_K = 7600Hz exceeded the Nyquist frequency of 4800Hz for the hotwire. Therefore, not all scales experiencing dissipation during the frontal passage could be resolved. The highest wind speed that allows resolution of a Kolmogorov microscale of 0.25mm with a MICROFRONTS anemometer sampling at 9600Hz is about 7 ms^{-1}. This threshold is noted on the first panel of Figure 1 to emphasize that direct dissipation calculations are inaccurate for wind speeds exceeding this threshold.

2.1 *The Cold front*

A dry Arctic cold front passed the MICROFRONTS site at approximately 0237 UTC (2037 LST) 20 March 1995, two hours after local sunset at 1839 LST. Time series spanning the period 0000-0600 UTC MICROFRONTS are shown in Figure 1.The 6-hr time period was chosen because it allows time for the front to completely pass the instrumented tower, with time on either side to view the state of the surface layer. The top two panels show wind speed and wind direction from the 10m south tower sonic anemometer, at a rate of 10 samples s^{-1}.The next panel shows dry bulb temperature from the 10m south tower platinum resistance thermometer, also at 10 samples s^{-1}. The last panel shows two surface layer scaling parameters, the local friction velocity u^* and the Monin-Obukhov scaling parameter $\zeta = z/L$, where L is a local Obukhov length. Both u^* and ζ are calculated from fluxes from the sonic anemometer at the 3m level. These scaling parameters are calculated using 900-s averaging intervals, centered on the time of the frontal passage. The dotted lines in Figure 1 delimit the frontal zone.

Note, visually, the sharp increase in wind speed variance with the passing of the front. After the front passes, the wind speed and speed variance decay to near prefrontal values. The wind has a southwesterly component in the prefrontal period. The temperature trace in panel 3 shows that there was a 2^{o}C rise in temperature starting at 0200 UTC, possibly due to advection of warmer air from the southwest or increased mixing in the surface layer. After the frontal passage, temperature decreased steadily due to radiational cooling and cold air advection. The wind shift and temperature drop were not coincident in this front, with the temperature drop at 10m lagging the wind shift by about 180s. This is also observed in Taylor et al. (1993) and Shapiro et al. (1985), suggesting that this front may have an elevated head, like a density current.

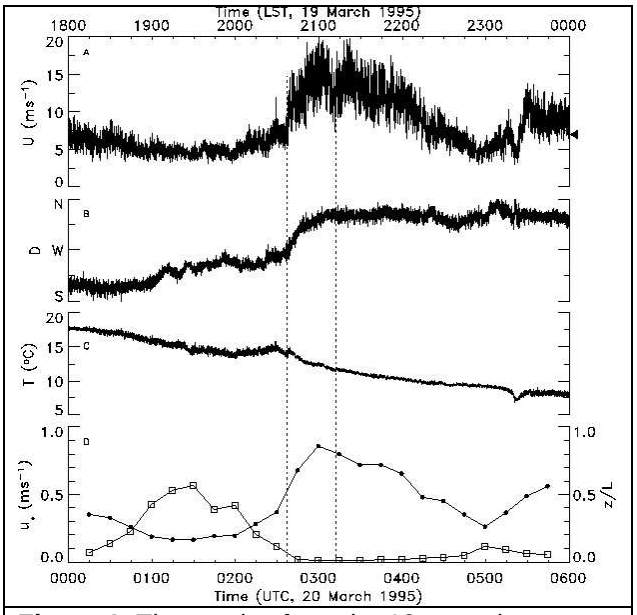

Figure 1: Time series from the 10m south tower instruments on 20 Mar 1995. (A) Wind speed from the sonic anemometer. The arrowhead on the right marks 7 ms^{-1}, the threshold for the hotwire anemometer to resolve the Kolmogorov microscale. (B) Wind direction from the sonic anemometer. (C) Temperature from the platinum resistance thermometer. (D) The friction velocity u^* (**.**) and the Monin-Obukhov scaling parameter ζ (squares). The dotted lines give the extent of the frontal zone.

3. DISSIPATION RATE CALCULATIONS

Dissipation rate was measured directly with the hotwire anemometer and calculated, using two inertial range techniques, with data collected from the sonic and hotwire anemometers.

A quantitative comparison between the estimated and directly calculated values of ε provides a test of the relative value of the inertial range estimates under varying turbulence and stability conditions.

3.1 *The direct dissipation technique (HD)*

Under the assumption of local isotropy, since there is no preferred direction, the tensorial form of

the mean turbulent kinetic energy dissipation rate ε reduces to a form that includes only a single velocity derivative (Tennekes and Lumley 1972): Because velocity derivative terms are involved, the correct instrument to use is the hotwire anemometer, since it is one of the few instruments capable of resolving the sharp gradients that occur at the smallest scales of turbulent motion.

A derivative series is constructed by differentiating the hotwire wind speed series. The derivative series is lowpass filtered at the noise floor of the hotwire anemometer. The square of the derivative series is then calculated over nonoverlapping 6s intervals. The Heskestad/Lumley correction factor in ranged between 5 and 10

Direct calculations of ε are not possible at all times during the frontal passage. The values of ε calculated when wind speeds are above 7ms-1 are still displayed, yet it is noted that they are incorrect because of this systematic error.

3.2 *The inertial dissipation technique (HI, SI)*

As described, for example, in Champagne et al. (1977), if $S_{u_i}(f)$ is the frequency spectrum of velocity component u_i in the inertial range and α_i is the Kolmogorov constant for the velocity component, the dissipation rate is given by

$$\varepsilon = \frac{2\pi}{U}\left(\frac{f^{5/3}S_{u_i}(f)}{\alpha_i}\right)^{3/2}.$$

This technique can be used by any sensor that has a sufficiently high frequency response to measure velocities in the inertial range (Oncley et al. 1996). Here, wind speed data from the sonic and hotwire anemometers are used to estimate ε with this technique.

3.3 Kolmogorov's four-fifths law (HK)

Another method for calculating dissipation rate is Kolmogorov's four-fifths law, an exact relation derived directly from the Navier-Stokes equations using the assumptions of homogeneity and isotropy. The four-fifths law gives an appealing method for estimating dissipation rate because there are no undetermined coefficients. Sreenivasan and Antonia (1997) suggest that the four-fifths law may provide a less ambiguous estimate of ε than the direct method and that it can also be used to fix the extent of the inertial subrange. Taylor's hypothesis is used to convert the four-fifths law to the time domain. Estimates of ε were made in 60s intervals with the hotwire anemometer data.

3.4 *Dissipation rate comparisons*

Figure 2 shows the inertial dissipation calculation and the calculation from Kolmogorov's four-fifth's law using data from the hotwire anemometer for the 6-hr analysis period surrounding the frontal passage. Figure 3 shows the direct dissipation calculation using data from the hotwire anemometer and the inertial dissipation calculation using data from the 3m sonic anemometer (SI) for the same period. Error bars depict 95 percent confidence intervals on each value of ε; see Piper (2001) for a treatment of the error analysis.

These Figures show that there is an order of magnitude increase in ε with this frontal passage. Also, there is fidelity between the four ε calculations, even though the direct method was untenable in high wind speed conditions. Note that the inertial dissipation technique from the sonic anemometergives reasonable values for ε even though an inertial range is not technically achieved.

The confidence intervals for the HI and HK calculations displayed in Figure 2 are small, even during the frontal passage, indicating random errors are controlled well. The confidence intervals on the HD calculation are smaller than the plot symbols because of the large number of points used in the calculation in comparison to the tiny integral scales of the velocity derivative. The confidence intervals on the SI calculation are uncomfortably large. The confidence in these ε values could be increased by further averaging in time or by including more points in the average through more spectral bands. Another means by which the confidence could be increased is by including independent calculations of ε from the transverse velocity component of the sonic anemometer.

Ideally, the four calculations of ε (HD, HI, HK and SI) should yield the same value for the dissipation rate in each 60s time interval. However, due to systematic errors---for example, the hotwire frequency response limit in the HD calculation or the lack of true inertial subrange measurements in SI---and random errors, the four calculations do not give the same value in each interval.

Figure 4 shows scatter plots comparing the values of ε calculated with the four techniques over the six hour period. In each panel, the 1:1 line is used instead of a least squares line of regression because none of the ε calculations can be

considered independent for the purposes of regression. The 1:1 line gives the ideal limit of where the individual data points should lie on each scatter plot.

Because the HD method cannot be used in the front, HI is used instead for a basis of comparison with the other calculations. Figure 4 shows that the values of HK and SI are visibly well correlated with the values of HI, as evidenced by the agreement with the 1:1 line in each plot. The agreement is favorable even during the frontal passage. The scatter between the calculations tends to increase with increasing ε. The scatter between the methods is mostly due to random error, since increasing the averaging interval reduces the amount of scatter.

Quantitative comparisons of these methods are provided in Piper and Lundquist (2004). The highest degree of correlation is between the calculations made with the hotwire anemometer, presumably because the large number of inertial range measurements from the hotwire tends to reduce random errors. The inertial dissipation method from the sonic anemometer also compares fairly well with the hotwire anemometer calculations. This result is important because it shows that ε calculations can be made with a sonic anemometer that compare favorably with those made from a hotwire anemometer, and sonic anemometers are much sturdier and easier to use and maintain in the field (Oncley et al. 1996).

4. SUMMARY

Ground truth has been established for turbulence levels within a surface frontal transition zone, including measurements of turbulent kinetic energy dissipation rate. These results can be used in assessing the effects of friction in the surface layer in traditional semigeostrophic models of frontal collapse or in models with an ageostrophic feedback mechanism.

Direct and indirect methods for calculating dissipation rate are used on data collected before, during, and after the passage of a cold front. Both sonic and hotwire anemometers are utilized. The calculations from the direct and indirect methods are found to compare well, even though information from different scales of turbulence are used in the calculations, and despite the fact that the calculations are obtained using wind field measurements from different instruments. The agreement in the calculations suggests that the indirect methods can be used safely to calculate ε where no direct calculations of e are available. The dissipation rate in the surface layer is found to increase by an order of magnitude in the 20 March 1995 frontal passage to a maximum value of ~1.2 m^2s^{-3}, compared to prefrontal values of ~0.05 m^2s^{-3}. Dissipation rate levels remain high even after the passage of the frontal zone.

Acknowledgements

Support for MP has been provided by the Air Force Office of Scientific Research under Grant F49620-95-1-014-1 and under AASERT Grant F49620-97-1-0448. Support for MP and JKL at the University of Colorado has been provided by the Atmospheric Sciences Division, Mesoscale Dynamcis Program of the National Science Foundation under Grant ATM-9903645. MP also thanks Research Systems, Inc. for allowing a leave of absence. This work was performed under the auspices of the U.S. Department of Energy by the University of California, Lawrence Livermore National Laboratory under contract No. W-7405-Eng-48.

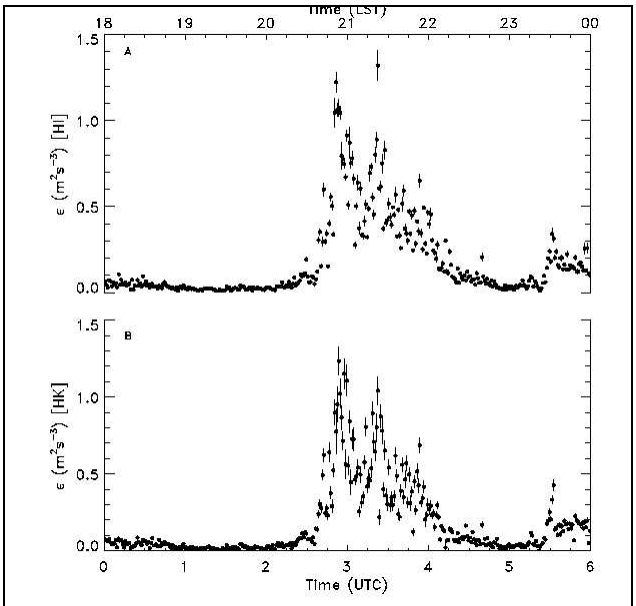

Figure 2: Dissipation rate calculations from the 3m hotwire anemometer for the 20 Mar 1995 front. Values of ε are calculated in 60s intervals. Error bars denote 95% confidence intervals on the means. (A) Inertial dissipation technique (HI). (B) Kolmogorov's fourth-fifth's law (HK).

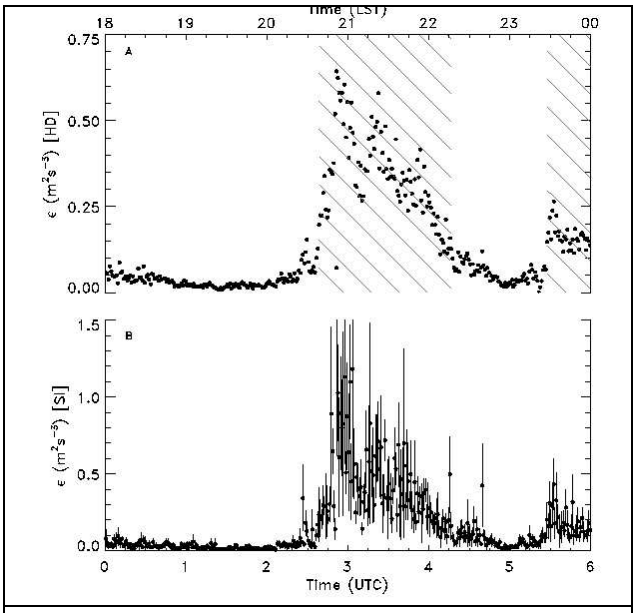

Figure 3: Dissipation rate calculations from the 3m hotwire and sonic anemometers for the 20 Mar 1995 front. Values of ε are calculated in 60s intervals. Error bars denote 95% confidence intervals on the means. (A) Direct dissipation technique from the hotwire (HD) ; note the expanded ordinate. The error bars are smaller than the plot symbols. The hatched areas indicate when wind speed exceeds 7 ms^{-1}. (B) Inertial dissipation techniques from the sonic (SI).

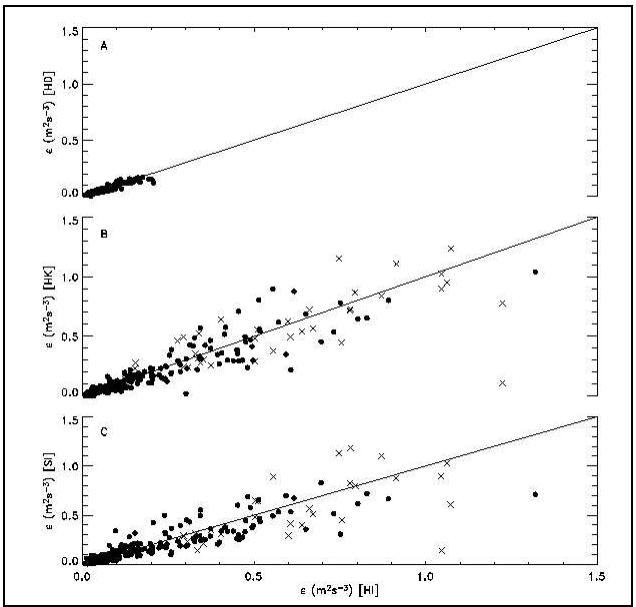

Figure 4: Scatterplots of the 60s ε calculations for the 20 Mar 1995 front. Symbols refer to calculations made within the frontal zone (x) and before and after the front (.). The solid lines show a 1:1 correspondence in the ε values. (A) Comparison between inertial dissipation (HI) and direct dissipation HD) calculations from the hotwire anemometer. The comparison is only made for wind speeds less than 7 ms^{-1}. (B) Comparison between inertial dissipation (HI) and Kolmogorov's four-fifth's law (HK) calculations from the hotwire anemometer. (C) Comparison between inertial dissipation calculations from the hotwire (HI) and sonic (SI) anemometers.

References

Blumen, W. and M. Piper, 1999: The frontal width problem. *J. Atmos. Sci.*, **56**, 3167-3172.

Chapman, D., and K.A. Browning, 2001: Measurements of dissipation rate in frontal zones. *Quart. J. Roy. Meteor. Soc.*, **127**, 1939-1959.

Champagne, F.H., C.A. Friehe, J.C. LaRue, and J.C. Wyngaard, 1977: Flux measurements, flux estimation techniques, and fine-scale turbulence measurements in the unstable surface layer over land. *J. Atmos. Sci.*, **34**, 515-530.

Champagne, F.H., 1978: The fine-scale structure of the turbulent velocity field. *J. Fluid. Mech*., **86**, 67-108.

Frank, H.P., 1994: Boundary layer structure in two fronts passing a tower. *Meteor. Atmos. Phys.*, **53**, 95-109.

Frish, U., 1995. *Turbulence: The Legacy of A. N. Kolmogorov*. Cambridge University Press, 296 pp.

Kennedy, P.J. and M.A. Shapiro, 1975: The energy budget in a clear air turbulence zone as observed by aircraft. *Mon. Wea. Rev.,* **103**, 650-654.

Oncley, S.P., C.A. Friehe, J.A. Businger, E.C. Itsweire, J. C. LaRue and S.S. Chang, 1996: Surface-layer fluxes, profiles, and turbulence measurements over uniform terrain under near-neutral conditions. *J. Atmos. Sci.*, **53**, 1029-1044.

Piper, M., 2001: The Effects of a Frontal Passage on Fine-Scale Nocturnal Boundary Layer Turbulence. Ph.D. dissertation, University of Colorado at Boulder, Dept. of Astrophysical, Planetary, and Atmospheric Sciences, 217 pp.

Piper, M., and J. K. Lundquist, 2004: Surface-Layer Turbulence Measurements during a Frontal Passage. *J. Atmos. Sci.*, to appear.

Pope, S. B., 2000. *Turbulent Flows.* Cambridge University Press, 771 pp.

Shapiro, M.A., T. Hampel, D. Rotzoll, and F. Mosher, 1985: The frontal hydraulic head: A micro-α scale (~1 km) triggering mechanism for mesoconvectiv weather systems. *Mon. Wea. Rev.*, **113**, 1166-1183.

Sreenivasan, K.R. and R. Antonio, 1997: The phenomenology of small-scale turbulence. *Annu. Rev. Fuild Mech.*, **29**, 435-472.

Taylor, P.A., J.R. Salmon, and R.E. Stewart, 1993: Mesoscale observations of surface fronts and low pressure centres in Canadian East Coast storms. *Bound.-Layer Meteorol.*, **64**, 15-54.

Tennekes, H., and J.L. Lumley, 1972: *A First Course in Turbulence.* The MIT Press, 300 pp.